JGP Journal of General Physiology

ARTICLE

Cooperative mechanisms underlie differences in myocardial contractile dynamics between large and small mammals

Jitandrakumar R. Patel[1], Kayla J.V. Park[3], Aidan S. Bradshaw[3], Tuan Phan[2], and Daniel P. Fitzsimons[3]

Ca^{2+} binding to troponin C (TnC) and myosin cross-bridge binding to actin act in a synergistic cooperative manner to modulate myocardial contraction and relaxation. The responsiveness of the myocardial thin filament to the activating effects of Ca^{2+} and myosin cross-bridge binding has been well-characterized in small mammals (e.g., mice). Given the nearly 10-fold difference in resting heart rates and twitch kinetics between small and large mammals, it is unlikely that the cooperative mechanisms underlying thin filament activation are identical in these two species. To test this idea, we measured the Ca^{2+} dependencies of steady-state force and the rate constant of force redevelopment (*k*tr) in murine and porcine permeabilized ventricular myocardium. While murine myocardium exhibited a steep activation-dependence of *k*tr, the activation-dependent profile of *k*tr was significantly reduced in porcine ventricular myocardium. Further insight was attained by examining force–pCa and *k*tr–pCa relationships. In the murine myocardium, the pCa_{50} for *k*tr was right-shifted compared with the pCa_{50} for force, meaning that increases in steady-state force occurred well before increases in the rate of force redevelopment were observed. In the porcine myocardium, we observed a tighter coupling of the force–pCa and *k*tr–pCa relationships, as evidenced by near-maximal rates of force redevelopment at low levels of Ca^{2+} activation. These results demonstrate that the molecular mechanisms underlying the cooperative activation of force are a dynamic property of the mammalian heart, involving, at least in part, the species- and tissue-specific expression of cardiac myosin heavy chain isoforms.

Introduction

Across mammalian species, regulation of myocardial contraction appears to be a highly cooperative process (Fitzsimons and Moss, 2007; Gillis et al., 2007; Solís and Solaro, 2021), initiated by the binding of Ca^{2+} to troponin C (TnC) and mediated by a series of events that results in the strong binding of myosin cross-bridges to actin and the development of force. Evidence for the cooperative activation of force has been obtained in permeabilized myocardial preparations where the kinetics of force development have been shown to scale with Ca^{2+} activation in small and large mammals (Édes et al., 2007; Stelzer et al., 2008; Giles et al., 2019; McDonald et al., 2020). Several mechanisms have been proposed to account for the activation dependence of force development, including a role of Ca^{2+} per se to increase the rate of cross-bridge attachment to actin (Landesberg and Sideman, 1994; Regnier et al., 2004) and a cooperativity-induced slowing of force development at low levels of Ca^{2+} activation (Campbell, 1997; Campbell et al., 2001). In Campbell's model, Ca^{2+} binding to TnC activates the associated troponin–tropomyosin functional unit spanning seven actin monomers, thus increasing the probability of myosin binding. The binding of myosin cross-bridges within the activated functional unit then cooperatively recruits further cross-bridge binding in near-neighbor units. While Ca^{2+} binding initiates the activation of the thin filament, the subsequent cooperative binding of cross-bridges amplifies and extends the activation profile along the thin filament (Razumova et al., 2000; Campbell et al., 2001; Lehrer and Geeves, 2014; Desai et al., 2015; Moore et al., 2016; Solís and Solaro, 2021). At low levels of Ca^{2+} activation, the kinetics of force development are slowed due to the time taken for the cooperative spread of cross-bridge binding and subsequent iterative activation of near-neighbor functional units. At saturating Ca^{2+}, the rate of force development is maximal since virtually all the functional units are activated by Ca^{2+} binding and the rate of force development manifests the maximal rate of cross-bridge cycling.

The dynamic regulation of contractility on a beat-to-beat basis is a hallmark feature of the mammalian heart which

[1]Department of Cell and Regenerative Biology, University of Wisconsin School of Medicine and Public Health, Madison, WI, USA; [2]Institute for Modeling Collaboration and Innovation, University of Idaho, Moscow, ID, USA; [3]Department of Animal, Veterinary, and Food Sciences, College of Agricultural and Life Sciences, University of Idaho, Moscow, ID, USA.

Correspondence to Daniel P. Fitzsimons: dfitzsimons@uidaho.edu.

matches cardiac output to the circulatory demands of peripheral tissues. The control systems that regulate myocardial contractility include autonomic inputs to the heart and circulating catecholamines working through second-messenger signaling pathways. Variations in sympathetic and parasympathetic activity elicit changes in the rate (chronotropy) and strength (inotropy) of contraction via protein kinase A-mediated phosphorylation of contractile and Ca^{2+} handling proteins. Given the nearly 10-fold difference in heart rate and myocardial twitch kinetics between small and large mammals, it is not surprising that the cardiac contractile and regulatory proteins differ among mammalian species. For example, all mammals express the α- and β-isoforms of the cardiac myosin heavy chain (MyHC), but the ratios and enzymatic activities of the ventricular MyHC isoforms vary in a species-dependent fashion. In the murine ventricle, the predominant isoform is the α-MyHC (Sadayappan et al., 2009), conferring both speed and power to the heart. In contrast, the ventricles of larger mammals predominantly express the β-MyHC isoform (Reiser et al., 2001), which exhibits much slower ATP turnover kinetics and lower contraction kinetics than α-MyHC (Deacon et al., 2012; Walklate et al., 2016, 2021).

The present study was undertaken to assess whether the species-specific expression of thick and thin filament proteins alters the cooperative activation of the myocardial thin filament. We propose that the responsiveness of the myocardial thin filament to the activating effects of Ca^{2+} and myosin cross-bridges is a dynamic property of the heart that differs in small (e.g., mouse) and large (e.g., swine) mammals. To test this idea, we measured the activation-dependence of the rate of force development and the Ca^{2+}-sensitivities of steady-state force and *k*tr in permeabilized myocardial preparations isolated from murine ventricles and porcine atria and ventricles. Compared with murine ventricular and porcine atrial myocardium, we observed significantly slower contraction kinetics in porcine ventricular myocardium. However, we found that the activating effects of Ca^{2+} and cross-bridge binding on contraction kinetics were significantly greater in porcine ventricular myocardium, due at least in part to a greater reliance on cooperative regulatory processes.

Materials and methods

Tissue

Murine ventricular tissue

Nine 129S1/Svlmj mice (Jackson Laboratory) of either sex (3–6-mo-old) were injected with 5,000 U heparin/kg body weight and euthanized with isoflurane. Each heart was rapidly excised, and the left and right ventricles were separated at the septum in Ca^{2+}-free Ringer's solution (in mM: 118 NaCl, 25 HEPES, 11 glucose, 4.8 KCl, 1.2 Na_2HPO_4, and 1.2 $MgSO_4$, pH 7.4 and 22°C). The ventricles were snap-frozen in liquid N_2 and stored at −80°C until used. All procedures for animal care, handling, and use were reviewed and approved by the University of Idaho Animal Care and Use Committee.

Porcine atrial and ventricular tissue

Myocardial samples (dimensions: 1 cm × 1 cm × 1 cm) of the ventricular base, apical, and mid-wall myocardium (Lang et al., 2005) and atrial tissue were dissected from four adult pigs (two of each sex, each weighing ∼45 kg) following euthanasia. The use of adult pigs was approved by the University of Wisconsin Medical School Animal Care and Use Committee. All ventricular and atrial tissue samples were snap-frozen in liquid N_2, individually wrapped in aluminum foil, and stored at −80°C until used. Myocardial tissue samples were generously provided by Dr. Richard Moss (University of Wisconsin). Steady-state mechanical measurements were conducted using three to four atrial and three to four ventricular myocardial samples per heart.

Steady-state mechanical measurements

Solutions

Solution compositions were calculated using the computer program of Fabiato (1988) and stability constants (Godt and Lindley, 1982) corrected to pH 7.0 and 22°C. The composition of the relaxing solution was (in mM) 100 KCl, 20 imidazole, 4 MgATP, 2 ethylene glycol-bis(2-aminoethyl ether)-*N*,*N*,*N*′,*N*′-tetraacetic acid (EGTA), and 1 free Mg^{2+}. The composition of the preactivating solution was (in mM) 100 N,N-bis(2-hydroxyethyl)-2-aminoethanesulfonic acid (BES), 15 creatine phosphate (CP), 5 dithiothreitol (DTT), 4 MgATP, 1 free Mg^{2+}, and 0.07 EGTA. Ca^{2+}-activating solutions contained (in mM) 100 BES, 15 CP, 7 EGTA, 5 DTT, 4 MgATP, and 1 free Mg^{2+}, with $[Ca^{2+}]_{free}$ ranging from 1 nM (i.e., pCa 9.0) to 32 µM (i.e., pCa 4.5). A range of submaximal pCa solutions containing differing $[Ca^{2+}]_{free}$ were prepared by mixing appropriate volumes of pCa 9.0 and pCa 4.5 solutions. The ionic strength of preactivating and Ca^{2+}-activating solutions was adjusted to 180 mM using potassium propionate.

Isolation of myocardial tissue

On the day of use, small pieces of ventricular or atrial tissue were thawed in ice-cold relaxing solution and subsequently homogenized for 1–2 s using a Polytron homogenizer. The homogenates were centrifuged at 120 × *g* for 2 min. The pelleted multicellular preparations were permeabilized following resuspension in ice-cold relaxing solution containing 1% Triton-X100 (and 250 µg/ml saponin for murine samples) for 30 min. The preparations were washed twice in fresh, ice-cold relaxing solution and stored on ice prior to mechanical measurements.

Experimental apparatus

Before each mechanical experiment, an individual permeabilized myocardial preparation (dimensions: 700–1,200 × 150–250 µm) was trimmed and mounted between a force transducer (model 403; Aurora Scientific) and a high-speed length controller (model 322B; Aurora Scientific). The experimental apparatus was placed on the stage of an Olympus inverted microscope equipped with a 40× objective and CCTV camera. Light from a halogen lamp was used to illuminate the preparation. Bitmap images of the skinned myocardium were acquired using an AGP 4×/2× graphics card and associated software (ATI Technologies), and were used to measure sarcomere length and fiber dimensions during activation and relaxation. All experiments were performed at 22°C and at an initial sarcomere length of ∼2.20 µm in pCa 9.0

solution. Changes in force and length-controller position were sampled (16-bit resolution, DAP5216a; Microstar Laboratories) at 2.0 kHz using SLControl software (https://www.slcontrols.com). All data were saved to computer files for data analysis.

Preparation and use of NEM-S1

Myosin subfragment 1 (S1) was purified from rabbit fast-twitch skeletal muscle and modified with N-ethylmaleimide (NEM), as described previously (Swartz and Moss, 1992). A stock solution of NEM-S1 was prepared following overnight dialysis against a solution of 20 mM imidazole, pH 7.0, and 1 mM DTT. The concentration of NEM-S1 (e.g., 15–25 μM) was estimated by absorbance at 280 nm using a mass absorptivity of 0.75 and a molecular mass of 118,000 D for myosin S1. To avoid saturating the cooperative mechanisms with strong-binding cross-bridges, we used a suboptimal concentration of NEM-S1. Therefore, an experimental solution of 1 μM NEM-S1 was prepared immediately before use by first mixing equal volumes of 2× pCa 9.0 solution and the stock solution of NEM-S1 and then adding the appropriate volume of 1× pCa solution. Murine skinned-ventricular preparations were incubated in a solution of pCa 9.0 for 15 min to allow for NEM-S1 binding to actin, transferred to a preactivating solution for 2 min, and then into activating solutions of varying pCa (i.e., pCa 6.6–4.5) without NEM-S1 for 10–30 s to measure steady-state force and the kinetics of force development (Stelzer et al., 2006). After each mechanical measurement, the myocardial preparation was returned to the pCa 9.0 solution containing NEM-S1.

Rate of force redevelopment

The rate constant of force redevelopment (*k*tr) in skinned myocardium was assessed, as previously described (Giles et al., 2019). The measurement of *k*tr utilizes a rapid slack–restretch maneuver designed to dissociate bound myosin cross-bridges from actin in a steadily Ca^{2+}-activated preparation. Each permeabilized preparation was transferred from pCa 9.0 solution to preactivating solution and then into activating solutions of varying pCa (i.e., pCa 6.8–4.5) and allowed to develop a steady-state isometric force. The preparation was rapidly (<2 ms) slackened by 20% of its original length, followed by a brief period of unloaded shortening, after which the preparation was restretched rapidly (<2 ms) to its initial length. To ensure that the maximal numbers of cross-bridges were detached prior to the redevelopment of force after the mechanical restretch, we used different periods of unloaded shortening for myocardial preparations from murine ventricle and porcine atria (~14 ms) and porcine ventricle (~20 ms; Palmer and Kentish, 1998). Fig. 1 shows the production of steady-state force in a solution of pCa 4.5 in permeabilized myocardial preparations isolated from porcine atrial and porcine ventricular tissue. Force redevelopment following the slack–restretch maneuver reflects the rate of cross-bridge cycling between weakly bound and strongly bound force-generating states. A *k*tr–pCa relationship was obtained by first maximally activating a skinned myocardial preparation in a solution of pCa 4.5 and then in a series of submaximally activating solutions between pCa 6.8–5.4. To account for any run-down in maximal *k*tr, the myocardial preparation was activated in a solution of pCa 4.5 at the end of each experiment. The apparent rate constants of force redevelopment were estimated by a linear transformation of the half-time of force redevelopment, i.e., $k\text{tr} = 0.693/t_{1/2}$ (Fitzsimons et al, 2001a, 2001b; Giles et al, 2019).

Force–pCa relationship

During the measurements of the rate of force redevelopment, each myocardial preparation was bathed in solutions of varying pCa and allowed to develop steady-state isometric force. The difference between steady-state force and the force baseline after the 20% slack step was calculated as the total force at that specific pCa. The active force at a given pCa was obtained by subtracting Ca^{2+}-independent force (resting force), measured in a solution of pCa 9.0, from the total force. A force–pCa relationship was constructed by expressing submaximal Ca^{2+}-activated force (P) at each pCa as a fraction of maximal Ca^{2+}-activated force (P_o) determined at pCa 4.5, i.e., P/P_o. The force–pCa data were fit using the equation: $P/Po = [Ca^{2+}]^n/(k^n + [Ca^{2+}]^n)$, where n is the Hill coefficient and *k* is the $[Ca^{2+}]$ required for half-maximal activation (pCa_{50}).

Analysis of myosin isoform expression

Preparation of myofibrillar proteins

Myofibrillar proteins were extracted from murine ventricular, porcine atrial, and porcine ventricular frozen myocardium (Patel et al., 2017). In brief, the frozen ventricles were homogenized in fresh, ice-cold relaxing solution and centrifuged. The resulting pellet was resuspended in fresh, ice-cold relaxing solution containing 1% Triton X-100 for 30 min on ice and then centrifuged. For the murine myocardium, 0.25 mg/ml saponin was added along with Triton X-100 during the chemical skinning process. Each myofibrillar pellet was washed and centrifuged three times in fresh, ice-cold relaxing solution. The final myofibrillar pellet was solubilized in urea/thiourea sample buffer containing 8 M urea, 2 M thiourea, 75 mM DTT, 50 mM Tris-HCl, pH 6.8, and 0.03% bromophenol blue (Warren and Greaser, 2003).

SDS-PAGE: MyHC isoform expression

The relative expression of cardiac MyHC isoforms (i.e., α- and β-MyHC) in murine and porcine myocardium were resolved on 6% acrylamide gels (Fig. 2), as described previously (Warren and Greaser, 2003). The resolving gel (6% T, 2.6% C) contained 10% glycerol, 375 mM Tris, pH 8.8, and 0.1% sodium dodecyl sulfate (SDS). The stacking gel (2.95% T, 15% C) contained 10% glycerol, 130 mM Tris, pH 6.8, and 0.1% SDS. Diallytartaramide (DATD) was used as a cross-linker in these gels since it has been shown to facilitate the electrophoretic separation of the high molecular weight cardiac MyHC isoforms (Warren and Greaser, 2003). The upper reservoir buffer contained 400 mM glycine, 50 mM Tris-base (no pH adjustment), 0.2% SDS, and 5 mM DTT, while the lower running buffer contained 200 mM glycine, 25 mM Tris-base (no pH adjustment), 0.1% SDS, and 1 mM DTT. Electrophoresis was performed at 16 mA constant current for 4.0 h in the cold room. After completion of electrophoresis, the gel was

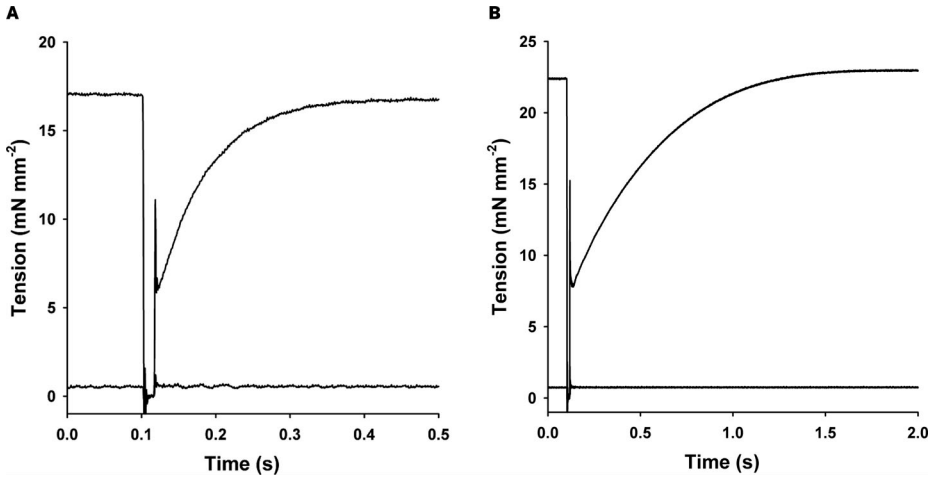

Figure 1. **Experimental protocol for determining steady-state tension and the kinetics of force redevelopment in mammalian skinned myocardium. (A and B)** Representative steady-state isometric tension data were obtained from permeabilized myocardial preparations isolated from the porcine left atrium (A) and porcine left ventricle (B) during maximal Ca^{2+} activation in a solution of pCa 4.5 (upper trace). Maximal Ca^{2+}-activated tension (P_o) was determined by subtracting Ca^{2+}-independent tension (P_{rest}) measured in a solution of pCa 9.0 (lower trace) from the total tension measured in the solution of pCa 4.5. Mechanical properties for porcine myocardium were as follows: atria (cross-sectional area = 2.2×10^{-8} m^2; P_o = 17.1 mN mm^{-2}; P_{rest} = 0.5 mN mm^{-2}; *k*tr = 14.8 s^{-1}) and ventricle (cross-sectional area = 3.5×10^{-8} m^2; P_o = 22.5 mN mm^{-2}; P_{rest} = 0.8 mN mm^{-2}; *k*tr = 2.4 s^{-1}).

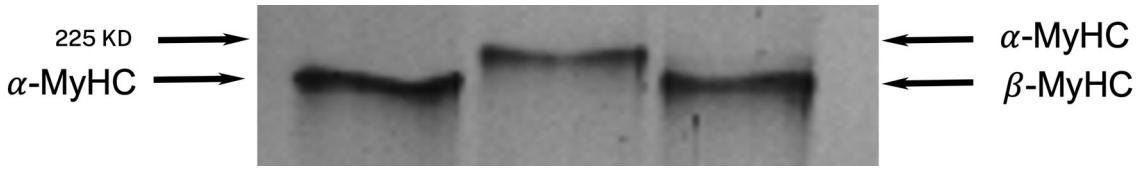

Figure 2. **Cardiac MyHC isoform expression in mammalian skinned myocardium.** A representative 6% SDS-PAGE illustrating the separation of α- and β-cardiac MyHC isoforms, which are identified by arrows in order of increasing electrophoretic mobility. Lane 1: murine ventricle, expressing predominantly α-MyHC; lane 2: porcine atria, expressing predominantly α-MyHC; and lane 3: porcine ventricle, expressing predominantly β-MyHC. Source data are available for this figure: SourceData F2.

silver stained (Patel et al., 2017) and the relative expression of cardiac MyHC isoforms was determined by densitometric analysis using Image Lab software (BioRad). The relative expression of α- and β-MyHC isoforms (expressed as a percentage of the total MyHC) was similar in murine ventricular (α: 97 ± 1%; β: 3% ± 1%) and porcine atrial (α: 98 ± 1%; β: 2% ± 1%) myocardium but differed from porcine ventricular myocardium (α: 7 ± 2%; β: 93% ± 3%).

Statistical analysis

All data are presented as means ± SEM. Statistical analyses were performed using a one-way ANOVA followed by the Holm–Sidak post hoc test for multiple comparisons with significance set at $P < 0.05$.

Results

Cooperative activation of force differs in murine and porcine myocardium

Permeabilized myocardial preparations isolated from murine ventricle, porcine atria, and porcine ventricle exhibited similar steady-state isometric force responses to activating Ca^{2+} (Fig. 3). The values of maximal Ca^{2+}-activated force (P_o), Ca^{2+}-independent force (P_{rest}), the Ca^{2+}-sensitivity of force (pCa_{50}), and the steepness of the force–pCa relationship (n_H) are summarized in Table 1.

Ca^{2+} and activation dependence of the rate of force redevelopment

Murine ventricular and porcine atrial myocardium exhibited similar steep Ca^{2+}-dependent increases in the rate constant of force redevelopment (Fig. 4 A). Increasing Ca^{2+} from threshold to maximal for force development increased *k*tr from 3.9 ± 0.7 s^{-1} at pCa 6.0 to 29.8 ± 2.1 s^{-1} at pCa 4.5 in murine ventricular myocardium and from 2.6 ± 0.2 s^{-1} at pCa 6.0 to 14.5 ± 0.8 s^{-1} at pCa 4.5 in porcine atrial myocardium. Although murine ventricular and porcine atrial myocardium each predominantly express the fast α-cardiac myosin (Fig. 2), the twofold difference in the maximal rates of force redevelopment in these tissues reflects species-specific enzymatic properties of the fast α-cardiac myosin (Yazaki et al., 1979; Malmqvist et al., 2004; Walklate et al., 2021). In porcine ventricular myocardium, *k*tr was found to vary with the level of Ca^{2+} activation but did so with a markedly shallow profile: mean *k*tr was 2.1 ± 0.2 s^{-1} at pCa 6.1, decreased to 0.9 ± 0.1 s^{-1} at pCa 5.8, and progressively

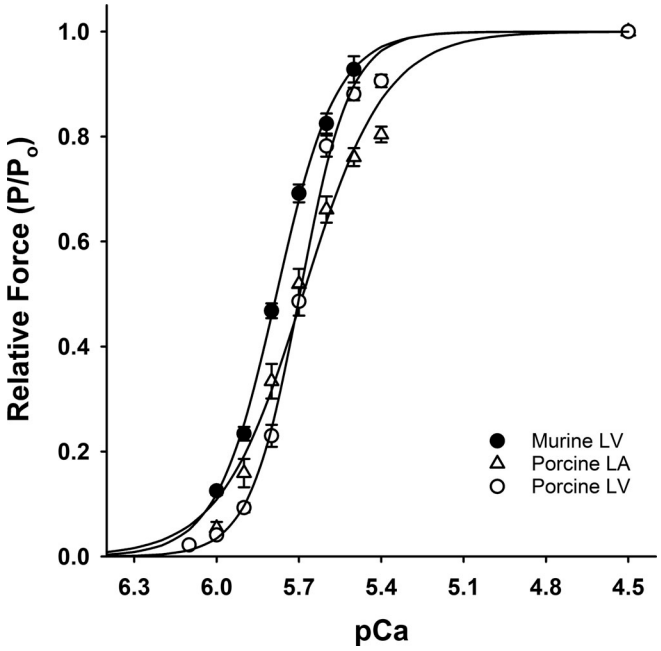

Figure 3. **Force–pCa relationships in mammalian skinned myocardium.** Force–pCa relationships were determined in permeabilized myocardial preparations. Smooth lines were generated by fitting the mean data with the Hill equation: $P/P_o = [Ca^{2+}]^n/(k^n + [Ca^{2+}]^n)$, where n is the Hill coefficient and k is the $[Ca^{2+}]$ required for half-maximal activation (i.e., pCa_{50}). Ca^{2+}-activated force–pCa relationships were determined in murine ventricular myocardium (filled circle: pCa_{50} = 5.78 ± 0.01, n_H = 4.0 ± 0.2), porcine atrial myocardium (triangle: pCa_{50} = 5.69 ± 0.02, n_H = 3.2 ± 0.2), and porcine ventricular myocardium (empty circle: pCa_{50} = 5.70 ± 0.01, n_H = 4.6 ± 0.1).

Table 1. **Summary of steady-state mechanical measurements**

Measurement	Murine LV (8) (Control)	Murine LV (7) (1 µM NEM-S1)	Porcine LA (12) (Control)	Porcine LV (15) (Control)
Po (mN mm^{-2})	21.5 ± 2.4	19.5 ± 1.9	22.6 ± 2.7	17.9 ± 0.9
P_{rest} (mN mm^{-2})	0.8 ± 0.1	1.3 ± 0.2	1.1 ± 0.3	0.5 ± 0.1
n_H	4.0 ± 0.2	3.6 ± 0.2	3.2 ± 0.1	4.6 ± 0.1[b]
pCa_{50}	5.78 ± 0.01	5.82 ± 0.02	5.69 ± 0.02[a]	5.70 ± 0.01[a]
k_{tr} (s^{-1})	29.8 ± 2.1	28.2 ± 2.1	14.5 ± 0.8[a]	2.9 ± 0.2[a,b]

All values are expressed as mean ± SEM, with the number of skinned myocardial preparations listed in parentheses. P_o, maximal Ca^{2+}-activated tension at pCa 4.5; P_{rest}, Ca^{2+}-independent tension at pCa 9.0; n_H, Hill coefficient for Ca^{2+}-activated force–pCa relationship; pCa_{50}, pCa required for half-maximal activation; k_{tr}, maximal rate of force redevelopment at pCa 4.5.
[a]Significantly different from control murine LV myocardium ($P < 0.05$).
[b]Significantly different from porcine atrial myocardium ($P < 0.05$).

increased to 2.9 ± 0.2 s^{-1} at pCa 4.5. The significant reduction in maximal *k*tr is due to the predominant expression of cardiac β-MyHC in porcine ventricular myocardium (Fig. 2). The rate constant of force redevelopment was also plotted as a function of steady-state isometric force, which was used as a measure of the level of thin filament activation due to the combination of Ca^{2+} binding to TnC and cooperative cross-bridge binding to actin. In both murine ventricular and porcine atrial myocardium, *k*tr increased as a function of increasing isometric force, gradually at low forces and rising more steeply at high forces (Fig. 4 B). However, to compare the activation-dependent profiles of *k*tr more appropriately (1) across species (murine ventricle versus porcine ventricle) and (2) within species (porcine atria versus porcine ventricle), *k*tr values recorded at each submaximal pCa were normalized to the maximal *k*tr value determined at pCa 4.5, i.e., ktr_{submax}/ktr_{max}, in each muscle type. Despite the significant differences in maximal absolute rates of force redevelopment, normalized *k*tr values for both the murine ventricular and porcine atrial myocardium exhibited a nearly identical steep activation-dependent profile (Fig. 5). In contrast, normalized *k*tr values were significantly faster in porcine ventricular myocardium, particularly at low and intermediate levels of Ca^{2+} activation (Fig. 5). At low levels of Ca^{2+} activation, *k*tr increased to levels approaching those measured during maximal activation in porcine ventricular myocardium. At intermediate levels of activation, normalized *k*tr values progressively decreased but were still significantly faster than values observed in murine ventricular and porcine atrial myocardium. The divergent activation-dependent profiles of *k*tr in murine and porcine myocardium support the hypothesis that unique species-specific contributions of thick and thin filament proteins underlie the cooperative regulatory processes in the mammalian heart.

Ca^{2+} sensitivities of steady-state force and the rate of force redevelopment in murine and porcine myocardium

Given the Ca^{2+} and activation dependence of *k*tr in mammalian myocardium, it was reasonable to assume that increases in $[Ca^{2+}]$ would result in parallel changes in force and the kinetics of force development. However, in both murine ventricular and porcine atrial myocardium (each expressing >95% α-cardiac myosin), the relationship between force development and pCa differed significantly from the *k*tr–pCa relationship in that the pCa_{50} for force was greater than the pCa_{50} for *k*tr, i.e., a higher $[Ca^{2+}]$ was required to achieve half-maximal activation of *k*tr (Fig. 6, A and B). In murine ventricular myocardium, the mean pCa_{50} for Ca^{2+}-activated force was 5.78 ± 0.01 compared to a mean pCa_{50} of 5.61 ± 0.02 for *k*tr (i.e., ΔpCa_{50} = 0.17 ± 0.01, $P < 0.05$). Similarly, in porcine atrial myocardium, the mean pCa_{50} for Ca^{2+}-activated force was 5.69 ± 0.02 as compared to a mean pCa_{50} of 5.46 ± 0.02 for *k*tr (i.e., ΔpCa_{50} = 0.22 ± 0.01, $P < 0.05$). However, the relationship between the Ca^{2+}-dependencies of force and *k*tr in the porcine ventricular myocardium was more tightly coupled. We observed that Ca^{2+}-dependent changes in steady-state force were accompanied by significant changes in the kinetics of force redevelopment. For example, at low $[Ca^{2+}]$, small increases in steady-state force were associated with near-maximal rates of force redevelopment (Fig. 6 C). The molecular basis of this observation most likely involves an enhanced degree of thin filament activation at low $[Ca^{2+}]$ in the porcine ventricular myocardium. With near maximal rates of force redevelopment at low levels of Ca^{2+}, the porcine ventricular thin

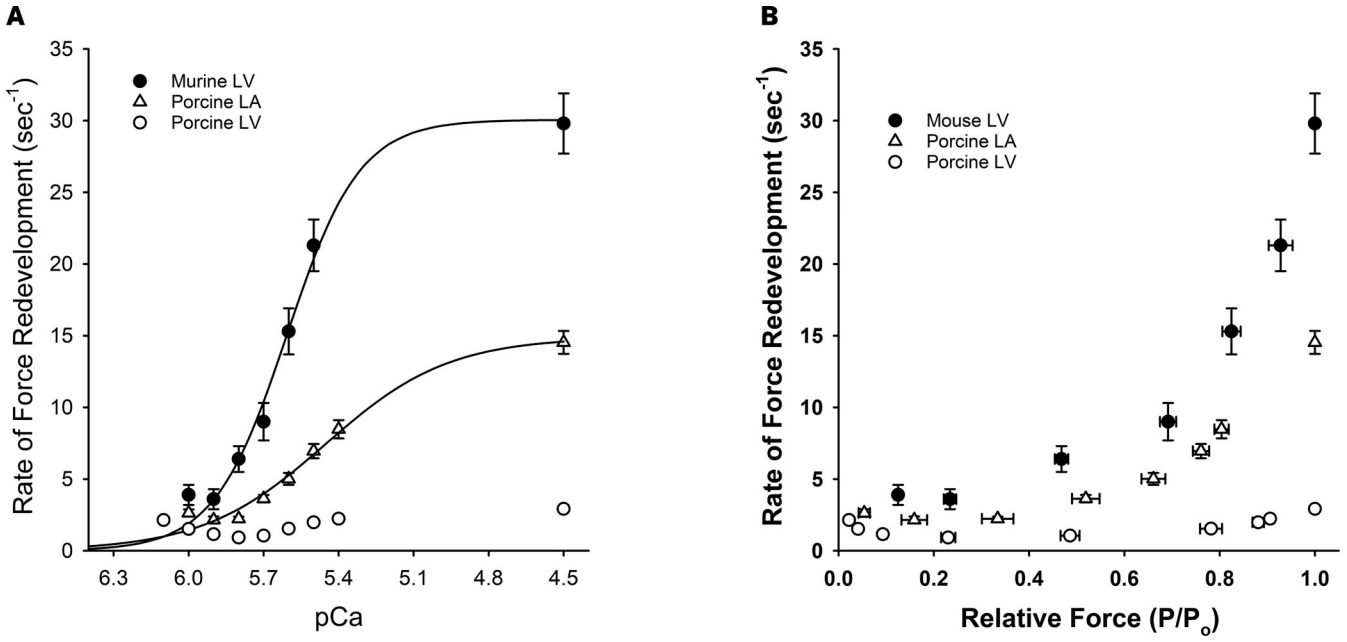

Figure 4. **The Ca^{2+} and activation dependence of the rate of force redevelopment in mammalian skinned myocardium.** The rate constant of force redevelopment (k_{tr}) following a rapid release/restretch maneuver was measured in permeabilized myocardial preparations isolated from murine ventricular myocardium (filled circle), porcine atrial myocardium (triangle), and porcine ventricular myocardium (empty circle). Data points represent means and the error bars are the SEM. **(A)** The Ca^{2+} dependence of the rate constant of force redevelopment. **(B)** The rate constant of force redevelopment was recorded as a function of relative steady-state force (P/P_o) measured at each pCa.

filament exhibits an augmented responsiveness to the activating effects of Ca^{2+} and myosin cross-bridges, such that further increases in $[Ca^{2+}]$ results in an increase in force but no further acceleration of the kinetics of force development.

Strongly bound cross-bridges increase the Ca^{2+} sensitivity of the rate of force redevelopment in murine myocardium

The steep activation dependence of *k*tr and the dissimilarity between the Ca^{2+} sensitivities of force and *k*tr in murine ventricular and porcine atrial myocardium could be explained by a cooperation-mediated slowing of cross-bridge binding at low levels of Ca^{2+} activation (Campbell, 1997; Campbell et al., 2001). If cross-bridge binding to the thin filament contributes to cooperative activation, then exogenous application of strongly bound cross-bridges should accelerate the rate of force redevelopment and reduce its dependence on the level of Ca^{2+} activation, as shown previously in skeletal muscle fibers and cardiac muscle preparations (Swartz and Moss, 1992; Fitzsimons et al., 2001a, 2001b; Stelzer et al., 2006). Therefore, we measured the rate of force redevelopment in murine permeabilized ventricular myocardial preparations in the presence of NEM-S1, a strong-binding analog of myosin S1 (Swartz and Moss, 1992). Treatment with NEM-S1 significantly reduced the Ca^{2+} and activation dependence of *k*tr in murine myocardium: mean *k*tr was 26.5 ± 2.2 s^{-1} at pCa 6.1, decreased to 14.7 ± 1.6 s^{-1} at pCa 5.8, and increased to 29.8 ± 2.1 s^{-1} at pCa 4.5 (Fig. 7 A). Furthermore, NEM-S1 treatment produced a significant leftward shift in the *k*tr–pCa relationship in murine myocardium (Fig. 7 B). Thus, treatment of murine ventricular myocardium with NEM-S1 accelerated the rate of force development at low and intermediate levels of Ca^{2+} activation and significantly increased the Ca^{2+} sensitivity of *k*tr in a manner comparable with that observed in untreated porcine ventricular myocardium.

Discussion

The mammalian heart exhibits significant beat-to-beat variations in the strength of myocardial contraction so that the circulatory demands of peripheral tissues are met (Moss et al., 2004). The beat-to-beat coordination of myocardial contractility and hemodynamic load is observed across the spectrum of mammalian species. The control systems that regulate ventricular contractility are multifaceted including neural and hormonal mechanisms (Moss et al., 2004). Nevertheless, these control systems ultimately regulate myocardial force development through highly interactive cooperative processes that vary depending upon the isoform expression of myosin and of regulatory proteins in the thin (troponin and tropomyosin) and thick (myosin binding protein-C) filaments. In all mammalian myocardium, Ca^{2+} binding to TnC triggers a series of interactions between the thick and thin myofilaments that result in the strong binding of myosin to actin and the subsequent development of force. Here, we tested the idea that cooperative activation of force in the hearts of small and large mammals is defined, in part, by the relative responsiveness of the thin filament to the activating effects of Ca^{2+} binding to troponin and strong binding of myosin cross-bridges to actin. Our results show that (1) the activation dependence of the rate of force

development, and (2) the degree of coupling between the Ca^{2+} sensitivities of force and the rate of force redevelopment (*k*tr) are species-specific properties of mammalian myocardium. These data suggest that thin filament responsiveness to the activating effects of Ca^{2+} and myosin cross-bridges modulates contractile kinetics and is an important determinant underlying the beat-to-beat regulation of ventricular contractility.

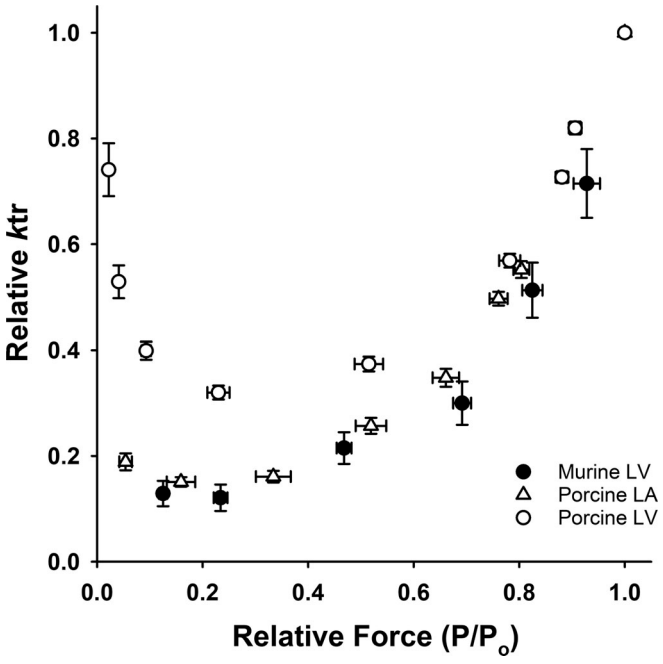

Figure 5. **The activation dependence of the rate of force redevelopment is significantly reduced in porcine-permeabilized ventricular myocardium.** The steady-state isometric forces and *k*tr values measured during submaximal Ca^{2+} activation were normalized to their respective maximal values measured in pCa 4.5 in permeabilized myocardial preparations isolated from murine ventricular myocardium (filled circle), porcine atrial myocardium (triangle), and porcine ventricular myocardium (empty circle). Data points represent means and the error bars are the SEM.

Activation dependencies of the rate of force redevelopment in murine and porcine myocardium—the role of strongly bound cross-bridges

In both murine ventricular and porcine atrial myocardium, the rate constant of force redevelopment increased nearly 10-fold when [Ca^{2+}] was increased from threshold to maximal values (Fig. 4). The steep activation dependence of *k*tr in these instances can be explained by a conceptual model that predicts a cooperation-mediated slowing of the rate of force development at low levels of Ca^{2+} activation (Campbell, 1997; Campbell et al, 2001; Moss et al, 2004; Fitzsimons and Moss, 2007). Upon Ca^{2+} binding to TnC, the associated troponin–tropomyosin functional unit is activated, which in turn increases the probability of myosin cross-bridge binding. According to the model proposed by Campbell (1997), myosin cross-bridges that bind to actin within this activated functional unit, cooperatively recruit myosin cross-bridge binding to actin in near-neighbor functional units (Gordon et al., 2000; Razumova et al., 2000; Campbell et al., 2001; Moore et al., 2016; Solís and Solaro, 2021; Mijailovich et al., 2021), which increases force but also prolongs the time-course of force development. As shown in Fig. 5, the activation dependence of *k*tr was much different in the porcine ventricular myocardium, which is evident in the near-maximal rates of *k*tr at low levels of Ca^{2+} activation. Regardless of species (murine versus porcine) or myocardial tissue source (porcine atria versus ventricle), Ca^{2+} binding to TnC is predicted to occur at discrete sites that are randomly distributed along the myocardial thin filament. However, the differential profiles of *k*tr across species and myocardial tissue strongly suggest that the responsiveness of the thin filament to the activating effects of Ca^{2+} and myosin cross-bridge binding is a dynamic modulator of contractile kinetics in mammalian myocardium.

A key question is what is the nature of the molecular mechanism underlying the enhanced level of thin filament

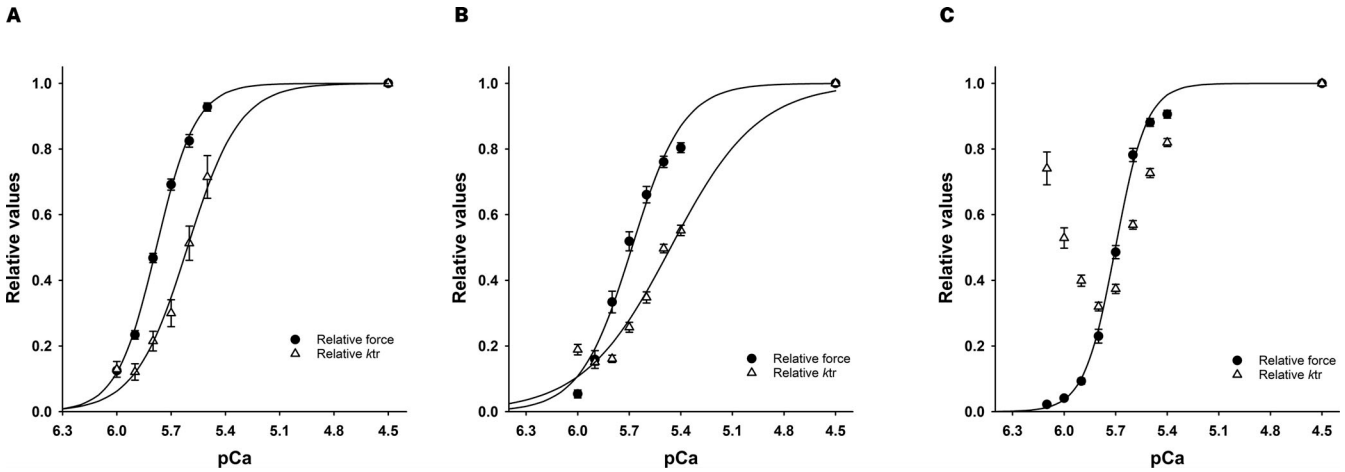

Figure 6. **The Ca^{2+} sensitivities of force and the rate of force redevelopment in mammalian skinned myocardium. (A–C)** Relative force–pCa (filled circle) and relative *k*tr–pCa (empty circle) relationships were determined in permeabilized myocardial preparations isolated from murine ventricular myocardium (A), porcine atrial myocardium (B), and porcine ventricular myocardium (C). Data points are means and the error bars are the SEM.

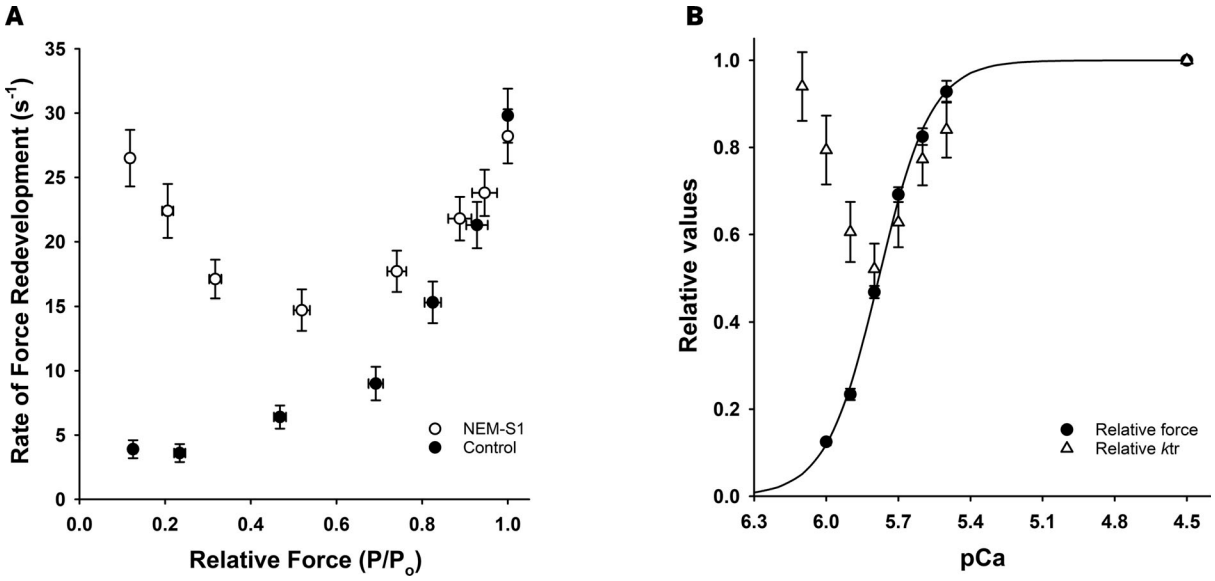

Figure 7. **Strong binding cross-bridges reduce the activation dependence of the rate of force redevelopment in murine ventricular myocardium.** The rate constant of force redevelopment was determined in the permeabilized murine ventricular myocardium in the absence (filled circle) and presence (empty circle) of 1 μM NEM-S1. Data points are means and the error bars are the SEM. **(A)** The rate constant of force redevelopment was recorded as a function of relative steady-state force (P/P_o) measured at each pCa. Note the significant increase in the rate of force redevelopment at low levels of Ca^{2+} activation following NEM-S1 treatment. **(B)** Relative force–pCa (filled circle) and relative *k*tr–pCa (empty circle) relationships were determined in permeabilized myocardial preparations isolated from murine ventricular myocardium following treatment with 1 μM NEM-S1. Data points are means and the error bars are the SEM.

activation in porcine ventricular myocardium? All mammals express the α and β isoforms of the cardiac MyHC in the healthy heart, but the ratios of the isoforms vary in a species- and tissue-dependent fashion. In murine myocardium, the principal (>95%) isoform is α-MyHC (Sadayappan et al., 2009), which has rapid ATP turnover kinetics, conferring both speed and power to the heart. In contrast, the ventricles of larger mammals predominantly (~90%) express the β-MyHC isoform (Reiser et al., 2001; Stelzer et al., 2008), which exhibits much slower ATP turnover kinetics and greater efficiency (lower rates of energy utilization) than α-MyHC (Locher et al., 2011). Compared with murine α-MyHC, human and porcine β-MyHCs exhibit a nearly 10-fold slower rate of ADP release (Deacon et al., 2012; Walklate et al., 2016, 2021), which could prolong the occupancy of β-MyHC bound to actin and thereby contribute to the cooperative recruitment of cross-bridges and activation of steady-state force. In the healthy porcine and human ventricular myocardium, we propose that the expression of a small amount of fast α-MyHC on a predominantly slow β-MyHC background in combination with strong near-neighbor regulatory unit (RU) interactions (Razumova et al., 2000; Kalda and Vendelin, 2020) provides the predominant molecular mechanisms underlying thin filament activation. Following Ca^{2+} binding to TnC, we propose that α-MyHC is the first to bind to the thin filament and because of its activating effects, α-MyHC opens the thin filament for initial β-MyHC binding and the subsequent cooperative spread of β-MyHC binding. At very low levels of Ca^{2+} activation, only a few thin filament RUs would be activated and have a strong cross-bridge bound. The presence of strong RU near-neighbor interactions would limit the cooperative spread of cross-bridge binding into neighboring RUs resulting in faster rates of force redevelopment at very low $[Ca^{2+}]$. As the $[Ca^{2+}]$ increases from low to intermediate levels, the likelihood of adjacent near-neighbor RUs having Ca^{2+} bound increases, making it more likely that another cross-bridge could bind within either RU or in a near-neighbor RU without Ca^{2+} bound. The time required for cooperative cross-bridge recruitment and subsequent binding will begin to slow *k*tr, reaching the minimum value that we observe at intermediate levels of Ca^{2+} (Fig. 5). As the $[Ca^{2+}]$ increases from intermediate to maximal levels, more RUs will have a Ca^{2+} bound leaving fewer RUs available for cooperative recruitment and *k*tr will progressively increase to maximal levels. Support for the actions of fast α-MyHC and slow β-MyHC is strengthened by the nearly identical activation-dependent profiles of contractile kinetics in murine ventricular and porcine atrial myocardium, which differ in their expression of thin filament proteins but are similar in their near-exclusive expression of fast α-MyHC. Furthermore, the exogenous application of strongly bound cross-bridges (i.e., NEM-S1) enhanced the level of thin filament activation in murine myocardium by accelerating the rate of force redevelopment and reducing its dependence on the level of Ca^{2+} activation (Fig. 7). It should be emphasized that the use of NEM-S1 substantially increased the number of strongly bound cross-bridges above that normally found in murine ventricular myocardium under normal physiological conditions. Thus, compared with porcine ventricular myocardium, it is likely that endogenous strongly bound cross-bridges are not as dominant in activating contractions in murine ventricular and porcine atrial myocardium, and that comparably weaker near-neighbor regulatory unit interactions mediated via thin filament regulatory proteins (e.g., troponin T and tropomyosin) play a proportionately greater role in the cooperative activation of force in these tissues.

The impact of the cooperative phenotype on ventricular functional capacity in the murine and porcine heart

The mechanical function of the mammalian ventricle can be adequately described by progressive changes in pressure and volume that occur within a single beat. While systole, ejection, diastole, and ventricular filling occur in both murine and porcine hearts, the timing of these events differs between them. At rest, the murine cardiac cycle is complete within ~100 ms but is nearly 10 times longer in the porcine heart (Tarkia et al., 2015). Given the short duration of the intracellular Ca^{2+} transient during a given myocardial twitch (Bers, 2002; Mijailovich et al., 2021), it is highly likely that thin filament activation and inactivation are significant determinants of ventricular systolic and diastolic function (Hanft et al., 2008; Solís and Solaro, 2021). At the level of the myocardium, this is clearly demonstrated by examining the relationship between the Ca^{2+}-dependencies of steady-state force and *k*tr. Under control conditions, we observed that the steady-state force–pCa relationship was left-shifted (i.e., required a lower $[Ca^{2+}]$ to achieve half-maximal activation) compared with the *k*tr–pCa relationship, indicating that increases in $[Ca^{2+}]$ resulted in the development of steady-state force well before significant increases in the kinetics of force development were observed (Fig. 6, A and B). In contrast, the porcine ventricle was characterized by a tighter coupling between force and *k*tr, such that Ca^{2+}-dependent increases in steady-state force were accompanied by marked increases in the rate of force development (Fig. 6 C).

In summary, force development and force relaxation in the mammalian heart result, at least in part, from the collective cooperative mechanisms underlying thin filament activation and inactivation. In murine ventricular myocardium, the steep activation dependence of *k*tr suggests a lesser reliance on cooperative mechanisms, which represents a physiological adaptation to a higher beat frequency and faster twitch kinetics. A lesser reliance on cooperative mechanisms provides the murine left ventricle the ability to respond to end-diastolic volume changes on the Frank–Starling curve but does so with a limited capacity to increase stroke volume for a given ventricular filling volume (Georgakopoulus and Kass, 2001), resulting in less-graded contractions. In contrast, the porcine ventricular myocardium exhibits a greater reliance on cooperative mechanisms in activating the kinetics of cross-bridge cycling. Such a mechanism in the ventricles of large mammals would generate a greater range in the strength and rate of force development during the cardiac cycle and provide means for optimizing the efficiency of contraction by fine-tuning the myocardial response to changes in circulatory load and inotropic stimulation.

Data availability

All data underlying this study are available in the published article.

Acknowledgments

Henk L. Granzier served as editor.

We thank Dr. Richard Moss for his generous gift of porcine myocardial tissue and for his helpful discussions and invaluable comments concerning this manuscript.

T. Phan acknowledges support from the National Institute of General Medical Sciences of the National Institutes of Health (grant P20GM104420).

Author contributions: D.P. Fitzsimons designed the study; J.R. Patel, K.J.V. Park, A.S. Bradshaw, and D.P. Fitzsimons collected the data; D.P. Fitzsimons and T. Phan analyzed the data; and D.P. Fitzsimons and J.R. Patel wrote the manuscript.

Disclosures: K. Park reported receiving a NASA ISGC grant for their fellowship with PI during the conduct of the study. No other disclosures were reported.

Submitted: 14 December 2022
Revised: 8 June 2023
Revised: 14 August 2023
Accepted: 29 August 2023

References

Bers, D.M. 2002. Cardiac excitation-contraction coupling. *Nature*. 415: 198–205. https://doi.org/10.1038/415198a

Campbell, K. 1997. Rate constant of muscle force redevelopment reflects cooperative activation as well as cross-bridge kinetics. *Biophys. J.* 72: 254–262. https://doi.org/10.1016/S0006-3495(97)78664-8

Campbell, K.B., M.V. Razumova, R.D. Kirkpatrick, and B.K. Slinker. 2001. Myofilament kinetics in isometric twitch dynamics. *Ann. Biomed. Eng.* 29:384–405. https://doi.org/10.1114/1.1366669

Deacon, J.C., M.J. Bloemink, H. Rezavandi, M.A. Geeves, and L.A. Leinwand. 2012. Erratum to: Identification of functional differences between recombinant human α and β cardiac myosin motors. *Cell. Mol. Life Sci.* 69: 4239–4255. https://doi.org/10.1007/s00018-012-1111-5

Desai, R., M.A. Geeves, and N.M. Kad. 2015. Using fluorescent myosin to directly visualize cooperative activation of thin filaments. *J. Biol. Chem.* 290:1915–1925. https://doi.org/10.1074/jbc.M114.609743

Édes, I.F., D. Czuriga, G. Csányi, S. Chlopicki, F.A. Recchia, A. Borbély, Z. Galajda, I. Édes, J. van der Velden, G.J.M. Stienen, and Z. Papp. 2007. Rate of tension redevelopment is not modulated by sarcomere length in permeabilized human, murine, and porcine cardiomyocytes. *Am. J. Physiol. Regul. Integr. Comp. Physiol.* 293:R20–R29. https://doi.org/10.1152/ajpregu.00537.2006

Fabiato, A. 1988. Computer programs for calculating total from specified free or free from specified total ionic concentrations in aqueous solutions containing multiple metals and ligands. *Methods Enzymol.* 157:378–417. https://doi.org/10.1016/0076-6879(88)57093-3

Fitzsimons, D.P., J.R. Patel, K.S. Campbell, and R.L. Moss. 2001a. Cooperative mechanisms in the activation dependence of the rate of force development in rabbit skinned skeletal muscle fibers. *J. Gen. Physiol.* 117: 133–148. https://doi.org/10.1085/jgp.117.2.133

Fitzsimons, D.P., J.R. Patel, and R.L. Moss. 2001b. Cross-bridge interaction kinetics in rat myocardium are accelerated by strong binding of myosin to the thin filament. *J. Physiol.* 530:263–272. https://doi.org/10.1111/j.1469-7793.2001.0263l.x

Fitzsimons, D.P., and R.L. Moss. 2007. Cooperativity in the regulation of force and the kinetics of force development in heart and skeletal muscles: Cross-bridge activation of force. *Adv. Exp. Med. Biol.* 592:177–189. https://doi.org/10.1007/978-4-431-38453-3_16

Georgakopoulos, D., and D. Kass. 2001. Minimal force-frequency modulation of inotropy and relaxation of in situ murine heart. *J. Physiol.* 534: 535–545. https://doi.org/10.1111/j.1469-7793.2001.00535.x

Giles, J., J.R. Patel, A. Miller, E. Iverson, D. Fitzsimons, and R.L. Moss. 2019. Recovery of left ventricular function following in vivo reexpression of cardiac myosin binding protein C. *J. Gen. Physiol.* 151:77–89. https://doi.org/10.1085/jgp.201812238

Gillis, T.E., D.A. Martyn, A.J. Rivera, and M. Regnier. 2007. Investigation of thin filament near-neighbour regulatory unit interactions during force development in skinned cardiac and skeletal muscle. *J. Physiol.* 580: 561–576. https://doi.org/10.1113/jphysiol.2007.128975

Godt, R.E., and B.D. Lindley. 1982. Influence of temperature upon contractile activation and isometric force production in mechanically skinned

muscle fibers of the frog. *J. Gen. Physiol.* 80:279–297. https://doi.org/10.1085/jgp.80.2.279

Gordon, A.M., E. Homsher, and M. Regnier. 2000. Regulation of contraction in striated muscle. *Physiol. Rev.* 80:853–924. https://doi.org/10.1152/physrev.2000.80.2.853

Hanft, L.M., F.S. Korte, and K.S. McDonald. 2008. Cardiac function and modulation of sarcomeric function by length. *Cardiovasc. Res.* 77:627–636. https://doi.org/10.1093/cvr/cvm099

Kalda, M., and M. Vendelin. 2020. Cardiac muscle regulatory units are predicted to interact stronger than neighboring cross-bridges. *Sci. Rep.* 10:5530. https://doi.org/10.1038/s41598-020-62452-7

Landesberg, A., and S. Sideman. 1994. Coupling calcium binding to troponin C and cross-bridge cycling in skinned cardiac cells. *Am. J. Physiol.* 266:H1260–H1271. https://doi.org/10.1152/ajpheart.1994.266.3.H1260

Lang, R.M., M. Bierig, R.B. Devereux, F.A. Flachskampf, E. Foster, P.A. Pellikka, M.H. Picard, M.J. Roman, J. Seward, J.S. Shanewise, et al. 2005. Recommendations for chamber quantification: A report from the American society of echocardiography's guidelines and standards committee and the chamber quantification writing group, developed in conjunction with the European association of echocardiography, a branch of the European society of cardiology. *J. Am. Soc. Echocardiogr.* 18:1440–1463. https://doi.org/10.1016/j.echo.2005.10.005

Lehrer, S.S., and M.A. Geeves. 2014. The myosin-activated thin filament regulatory state, M^{-}-open: A link to hypertrophic cardiomyopathy (HCM). *J. Muscle Res. Cell Motil.* 35:153–160. https://doi.org/10.1007/s10974-014-9383-z

Locher, M.R., M.V. Razumova, J.E. Stelzer, H.S. Norman, and R.L. Moss. 2011. Effects of low-level α-myosin heavy chain expression on contractile kinetics in porcine myocardium. *Am. J. Physiol. Heart Circ. Physiol.* 300:H869–H878. https://doi.org/10.1152/ajpheart.00452.2010

Malmqvist, U.P., A. Aronshtam, and S. Lowey. 2004. Cardiac myosin isoforms from different species have unique enzymatic and mechanical properties. *Biochemistry*. 43:15058–15065. https://doi.org/10.1021/bi0495329

McDonald, K.S., L.M. Hanft, J.C. Robinett, M. Guglin, and K.S. Campbell. 2020. Regulation of myofilament contractile function in human donor and failing hearts. *Front. Physiol.* 11:468. https://doi.org/10.3389/fphys.2020.00468

Mijailovich, S.M., M. Prodanovic, C. Poggesi, M.A. Geeves, and M. Regnier. 2021. Multiscale modeling of twitch contractions in cardiac trabeculae. *J. Gen. Physiol.* 153:e202012604. https://doi.org/10.1085/jgp.202012604

Moore, J.R., S.G. Campbell, and W. Lehman. 2016. Structural determinants of muscle thin filament cooperativity. *Arch. Biochem. Biophys.* 594:8–17. https://doi.org/10.1016/j.abb.2016.02.016

Moss, R.L., M. Razumova, and D.P. Fitzsimons. 2004. Myosin crossbridge activation of cardiac thin filaments: Implications for myocardial function in health and disease. *Circ. Res.* 94:1290–1300. https://doi.org/10.1161/01.RES.0000127125.61647.4F

Palmer, S., and J.C. Kentish. 1998. Roles of Ca^{2+} and crossbridge kinetics in determining the maximum rates of Ca^{2+} activation and relaxation in rat and Guinea pig skinned trabeculae. *Circ. Res.* 83:179–186. https://doi.org/10.1161/01.RES.83.2.179

Patel, J.R., G.P. Barton, R.K. Braun, K.N. Goss, K. Haraldsdottir, A. Hopp, G. Diffee, T.A. Hacker, R.L. Moss, and M.W. Eldridge. 2017. Altered right ventricular mechanical properties are afterload dependent in a rodent model of bronchopulmonary dysplasia. *Front. Physiol.* 8:840. https://doi.org/10.3389/fphys.2017.00840

Razumova, M.V., A.E. Bukatina, and K.B. Campbell. 2000. Different myofilament nearest-neighbor interactions have distinctive effects on contractile behavior. *Biophys. J.* 78:3120–3137. https://doi.org/10.1016/S0006-3495(00)76849-4

Regnier, M., H. Martin, R.J. Barsotti, A.J. Rivera, D.A. Martyn, and E. Clemmens. 2004. Cross-bridge versus thin filament contributions to the level and rate of force development in cardiac muscle. *Biophys. J.* 87:1815–1824. https://doi.org/10.1529/biophysj.103.039123

Reiser, P.J., M.A. Portman, X.-H. Ning, and C. Schomisch Moravec. 2001. Human cardiac myosin heavy chain isoforms in fetal and failing adult atria and ventricles. *Am. J. Physiol. Heart Circ. Physiol.* 280:H1814–H1820. https://doi.org/10.1152/ajpheart.2001.280.4.H1814

Sadayappan, S., J. Gulick, R. Klevitsky, J.N. Lorenz, M. Sargent, J.D. Molkentin, and J. Robbins. 2009. Cardiac myosin binding protein-C phosphorylation in a {beta}-myosin heavy chain background. *Circulation.* 119:1253–1262. https://doi.org/10.1161/CIRCULATIONAHA.108.798983

Solís, C., and R.J. Solaro. 2021. Novel insights into sarcomere regulatory systems control of cardiac thin filament activation. *J. Gen. Physiol.* 153:e202012777. https://doi.org/10.1085/jgp.202012777

Stelzer, J.E., D.P. Fitzsimons, and R.L. Moss. 2006. Ablation of myosin-binding protein-C accelerates force development in mouse myocardium. *Biophys. J.* 90:4119–4127. https://doi.org/10.1529/biophysj.105.078147

Stelzer, J.E., H.S. Norman, P.P. Chen, J.R. Patel, and R.L. Moss. 2008. Transmural variation in myosin heavy chain isoform expression modulates the timing of myocardial force generation in porcine left ventricle. *J. Physiol.* 586:5203–5214. https://doi.org/10.1113/jphysiol.2008.160390

Swartz, D.R., and R.L. Moss. 1992. Influence of a strong-binding myosin analogue on calcium-sensitive mechanical properties of skinned skeletal muscle fibers. *J. Biol. Chem.* 267:20497–20506. https://doi.org/10.1016/S0021-9258(19)88730-6

Tarkia, M., C. Stark, M. Haavisto, R. Kentala, T. Vähäsilta, T. Savunen, M. Strandberg, V.-V. Hynninen, V. Saunavaara, T. Tolvanen, et al. 2015. Cardiac remodeling in a new pig model of chronic heart failure: Assessment of left ventricular functional, metabolic, and structural changes using PET, CT, and echocardiography. *J. Nucl. Cardiol.* 22:655–665. https://doi.org/10.1007/s12350-015-0068-9

Walklate, J., Z. Ujfalusi, and M.A. Geeves. 2016. Myosin isoforms and the mechanochemical cross-bridge cycle. *J. Exp. Biol.* 219:168–174. https://doi.org/10.1242/jeb.124594

Walklate, J., C. Ferrantini, C.A. Johnson, C. Tesi, C. Poggesi, and M.A. Geeves. 2021. Alpha and beta myosin isoforms and human atrial and ventricular contraction. *Cell. Mol. Life Sci.* 78:7309–7337. https://doi.org/10.1007/s00018-021-03971-y

Warren, C.M., and M.L. Greaser. 2003. Method for cardiac myosin heavy chain separation by sodium dodecyl sulfate gel electrophoresis. *Anal. Biochem.* 320:149–151. https://doi.org/10.1016/S0003-2697(03)00350-6

Yazaki, Y., S. Ueda, R. Nagai, and K. Shimada. 1979. Cardiac atrial myosin adenosine triphosphatase of animals and humans: Distinctive enzymatic properties compared with cardiac ventricular myosin. *Circ. Res.* 45:522–527. https://doi.org/10.1161/01.RES.45.4.522